急冷 Cu-Sn 合金箔快速凝固连接工艺

翟秋亚， 杨金山， 徐锦锋， 郭学锋
（西安理工大学 材料学院，西安 710048）

翟秋亚

摘 要：应用微型电容储能焊机对厚度约 40～60 μm 的急冷 Cu-Sn 合金箔带进行了快速凝固焊接，分析了焊接工艺参数对接头组织与性能的影响. 结果表明，在储能电容不变的条件下，焊接电压及电极力对接头抗剪强度有着显著影响. 随着锡含量增加，实现合金箔焊接所需要的电压减小，电极力增大. Cu-7%Sn，Cu-13.5%Sn 合金箔比较适宜的焊接工艺参数分别为 U= 90 V，F= 11 N 及 U= 85 V，F= 11.5 N. 气孔是 Cu-Sn 合金箔主要焊接缺陷. 随电压降低或电极力增加，接头冷却速率增大，气相形核率降低，气泡长大、合并和迁移在一定程度上受到抑制，气孔产生降低.

关键词：急冷 Cu-Sn 合金；合金箔；快速凝固焊接；抗剪强度
中图分类号：TG456.9 文献标识码：A 文章编号：0253－360X(2009)07－0053－04

0 序 言

应用快速凝固技术可获得晶粒细小、固溶度扩展、偏析程度降低的合金材料[1－3]. 急冷 Cu-Sn 合金以其优异的物化性能和力学性能，在机械、微电子、化工和国防工业等领域具有广阔的应用前景[4－6]. 然而，快速凝固 Cu-Sn 合金有着典型的亚稳态结构特征，其焊接难度较大[3,5]. 应用电容储能、瞬间放电产生的大电流可以实现急冷合金箔材的点焊连接，接头组织具有典型的快速凝固特征[7－9]，有关 Cu-Sn 合金焊接接头的组织形态和熔核形成机制研究已经取得了一定的进展[9,10]. 而焊接工艺参数与接头组织及性能之间的相关性还有待于系统深入的研究. 文中应用微型电容储能焊机对急冷 Cu-Sn 合金箔带进行快速凝固焊接，研究焊接工艺参数对接头组织及力学性能的影响.

1 试验方法

Cu-x%Sn(质量分数，x=7，13.5)合金用高纯金属(99.99%)Cu 和 Sn 在超高真空电弧炉中熔配而成. 采用单辊法实现快速凝固，试验过程详见文献[4]，获得的合金箔厚度约 40～60 μm，宽约5 mm，长 1～2 m. 合金箔经丙酮清洗后，刮去其待焊表面上的毛刺，装配成搭接接头，在微型直流电容储能电阻焊机上进行点焊连接，连接方法详见文献[8]，焊接工艺参数如表 1 所示. 焊接接头样品经用树脂镶嵌和抛光后，选用“5 g $FeCl_3$＋15 mL HCl＋100 mL C_2H_5OH”溶液进行浸蚀. 用 XJG －05 型光学显微镜和 ARMRAY －1000B 型扫描电镜观测和分析接头的组织形态. 用 SH －500 数字推拉力计测试接头的抗剪强度.

表 1 储能焊工艺参数

Table 1 Welding parameters of CDW

电极力 F/N	焊接电压 U/V	充电电容 C/μF
9～15	80～100	3 300

2 结果及讨论

2.1 工艺参数对接头性能的影响

点焊接头力学性能通常用接头抗剪强度来表征. 接头的抗剪强度主要取决于焊接能量、电极力及焊接时间等工艺参数. 在焊接能量和焊接时间一定的情况下，电极力和焊接电压对接头抗剪强度有显著的影响. 文中主要讨论电极力及焊接电压对接头抗剪强度的影响.

2.1.1 电极力的影响

在焊接电压一定的条件下，Cu-Sn 合金焊接接

收稿日期：2008－12－29
基金项目：陕西省自然科学基金(2006E134，2006E120)；陕西省教育厅科学研究计划(06JK220)资助的课题

头抗剪强度随电极力的变化如图 1 所示. 可以看出, 随着电极力的增大, 接头抗剪强度逐渐升高, 达到最大值后又逐渐减小. 这是由于当电极力较小时, 待焊箔材之间的接触电阻较大, 接触电阻热造成界面微区金属过热氧化和蒸发, 引起飞溅并产生气孔. 如果将电极力进一步减小, 使其小于某一临界值, 接触界面将发生起弧现象, 甚至造成接头烧穿, 严重恶化接头力学性能. 随着电极力的增大, 位于两电极之间的合金箔材界面接触充分, 形成的熔核尺寸趋于稳定, 形态比较规则, 接头强度较高. 但是, 随着电极力的进一步增大, 接头抗剪强度反而下降. 其原因是, 较大的电极力导致待焊箔材界面接触电阻下降, 焊接能量不足而难于实现焊接. 即使实现了焊接, 也只能达成塑性连接而使接头性能明显降低, 如图 2 所示.

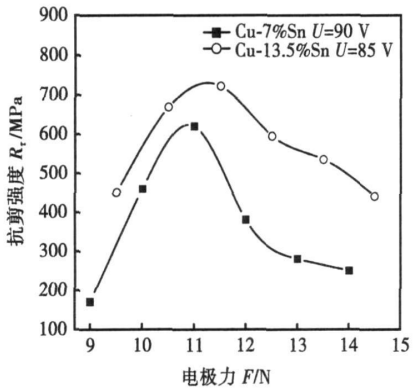

图 1 接头抗剪强度随电极力的变化

Fig. 1 Variations of joint shear strength with electrode pressure

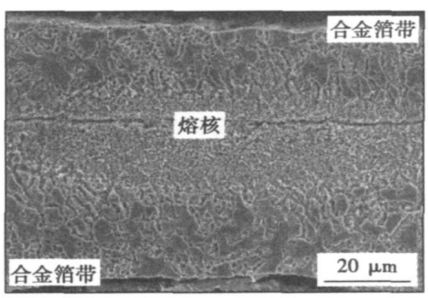

图 2 Cu-Sn 微型接头中的塑性连接

Fig. 2 Plastic joining of Cu-Sn micro-joint

另外, 随着锡含量增大, Cu-Sn 合金熔点降低, 实现其焊接所需要的能量也趋于降低; 合金箔带的电阻率增大, 对焊接电压的需求也趋于减小. 可见, 随锡含量的增加, 合金的熔点降低, 电阻率增大, 较低的焊接能量便能实现合金箔材的局部熔化而形成快速凝固连接接头. 急冷 Cu-Sn 合金快速凝固连接接头的抗剪强度较高. 在焊接电压分别为 90 V 和 85 V 时, Cu-7%Sn, Cu-13.5%Sn 连接接头的最大抗剪强度分别可达 608 MPa 和 730 MPa.

2.1.2 焊接电压的影响

在电极力一定的条件下, Cu-Sn 箔带焊接接头抗剪强度随焊接电压的变化如图 3 所示. 可以看出, 随着焊接电压升高, 接头抗剪强度先是由低增高、达到最高点后又逐渐减小. 这是由于电压较小时, 能量不足, 焊接区金属未能达到完全熔融, 获得的接头抗剪强度较低. 随着焊接电压的升高, 焊接热量增大, 熔核尺寸稳中有增, 接头强度不断提高. 但当焊接电压过高, 输入能量过大, 使两待焊箔材接触界面间的气隙击穿, 产生等离子体放电而引燃电弧, 导致熔化金属氧化和飞溅, 恶化接头质量, 降低接头的抗剪强度, 如图 4 所示.

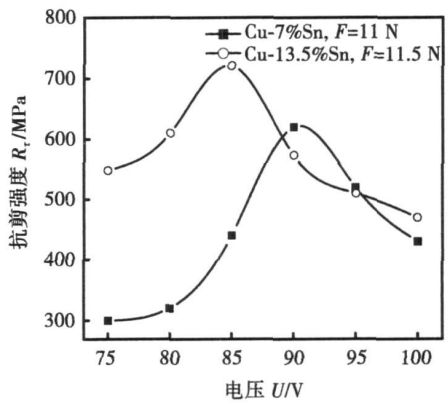

图 3 接头抗剪强度随电压的变化

Fig. 3 Variations of joint shear strength with welding voltage

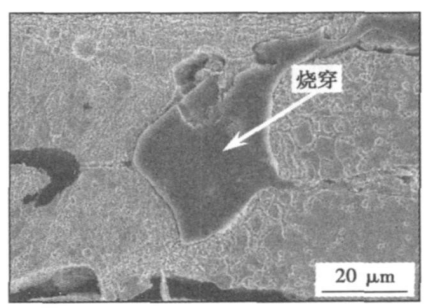

图 4 微型接头中的烧穿缺陷

Fig. 4 Burn-through in the micro-joint

随着 Sn 含量的增大, Cu-Sn 合金强度升高. 强度较高的合金其塑性变形抗力较大. 表现在焊接 Sn 含量高的 Cu-Sn 合金所需的电极力也随之增大. 当电极力为 11 N 和 11.5 N 时, Cu-7%Sn 和 Cu-13.5%

Sn 合金焊接接头抗剪强度分别达到最高值 608 MPa 和 730 MPa.

2.2　焊接缺陷及其影响因素

在焊接电容不变的条件下，焊接电压和电极力是影响接头接质量的两个主要因素，当工艺参数选择不当，快速凝固 Cu-Sn 合金连接接头容易出现缩孔和气孔缺陷.

2.2.1　缩孔及其影响因素

图 5 是焊接电压 85 V，电极力 10.5 N 时获得的焊接接头，从接头处可看到在熔核边缘偏近箔材接触界面处出现直径约为 8 μm 的近球形集中缩孔. 焊接过程中电极力大小是决定熔核中是否存在缩孔及缩孔大小的最重要因素. 因为缩孔是金属的收缩性缺陷，若熔核内液相不足以填满空间，便会在熔核的最后凝固处产生缺陷. 在硬规范储能焊过程中，焊区加热集中，熔核温度梯度大，加热和冷却速度均很大，处于过热状态的熔核被包围在塑性金属环和刚性金属之中，其液态收缩和凝固收缩势必导致缩孔的产生. 但在通常情况下，由于熔核凝固在电极力的持续作用下完成，压力造成的焊点周围金属的变形对减小和消除缩孔起到积极作用. 但是，倘若电极力过小，缩孔便不可避免.

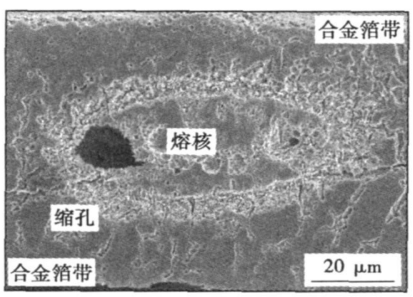

图 5　微型接头中的缩孔

Fig. 5　Shrinkage void in the micro-joint

2.2.2　气孔及其影响因素

试验发现，气孔是 Cu-Sn 合金快速凝固中最常见的焊接缺陷. 关于气孔的成因，Cu-Sn 合金中 Sn 含量对气孔大小及生成气孔的倾向性见文献[9, 10]. 文中主要从焊接工艺角度研究对气孔形成的控制.

焊接工艺参数(焊接电压、电极力)对气孔形成的影响是通过改变熔核凝固过程的冷却速率体现出来的. 当焊接电压升高，电极力减小时，接头处获得的焊接能量增大，熔核尺寸增大，冷却速率降低. 从文献[10]所示的温度场可知，熔核中心温度最高，冷却速率最低，冷却最为缓慢. 因此，可用熔核中心的冷却速率来表征接头的传热速度和凝固速率. 熔核尺寸越小，冷却速率越大，对熔核的凝固过程和气孔形成影响越显著. 理论计算获得的熔核中心冷却速率随熔核半径的变化如图 6 所示. 可知，随着熔核半径的增大，接头冷却速率迅速降低；而随着熔核半径的减小，接头冷速则大幅度升高. 在较高的冷却速率下，一方面，气孔的形核率低，气孔数量减小；另一方面，气孔的长大、合并和迁移在一定程度上被抑制，气孔分布具有一定的随机性. 图 7 为较高冷速下气孔在熔核中的分布情况. 可以看出，熔核中气孔数量相对较多，尺寸较小，随机地分布于熔核的整个断面.

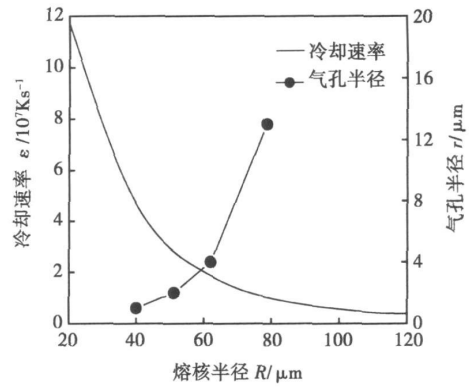

图 6　冷却速率和气孔半径随熔核半径的变化

Fig. 6　Cooling rate and porosity radius versus nugget radius

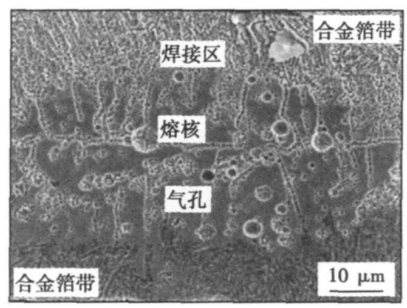

图 7　接头中的气孔

Fig. 7　Porosities in the micro-joint

3　结　　论

(1) 焊接工艺参数对接头力学性能有着显著的影响. 随 Sn 含量的升高，合金强度提高，电阻率增大，实现高强度连接所需要的焊接能量降低，电极力增大.

(2) Cu-Sn 合金箔带快速凝固连接接头具有较高的力学性能. 在焊接电压为 90 V 和 85 V、电极力

为11 N 和 11.5 N 时, Cu-7%Sn 和 Cu-13.5%Sn 合金箔带的焊接接头剪切强度分别达到最高值608 MPa 和730 MPa.

(3) 气孔是 Cu-Sn 合金快速凝固中最常见的焊接缺陷. 随着焊接电压降低或电极力的增加, 熔核半径的减小, 接头冷速增高, 气孔产生倾向降低.

参考文献:

[1] Lee K L, Hu C K. In situ scanning electron microscope comparison studies on electromigration of Cu and Cu(Sn) alloys for advanced chip interconnects[J]. Journal of Applied Physics, 1995, 78(7): 4428—4437.

[2] Liu X Y, Kane W, McMahon C J. On the suppression of dynamic embrittlement in Cu-8wt%Sn by an addition of zirconium[J]. Scripta Materilia, 2004, 50(5): 673—677.

[3] Huang J S, Zhang J, Cuevas A, *et al*. Recrystallization and grain growth in bulk Cu and Cu(Sn) alloy[J]. Materials Chemistriy and Physics, 1997, 49(1): 33—41.

[4] 翟秋亚, 杨 扬, 徐锦锋, 等. 快速凝固 Cu-Sn 亚包晶合金的电阻率及力学性能[J]. 物理学报, 2007, 56(10): 6118—6123.
Zhai Qiuya, Yang Yang, Xu Jinfeng, *et al*. Electrical resistivity and mechanical properties of rapidly solidified Cu-Sn hypoperitectic alloy [J]. Acta Phsica, 2007, 56(10): 6118—6123.

[5] Clevenger L A, Arcot B, Ziegler W, *et al*. Interdiffusion and phase formation in Cu(Sn) alloy films[J]. Journal of Applied Physics, 1998, 83(1): 90—99.

[6] Al-Ganainy G S, Fawzy A, Ei-Salam F A. Transient and steady—state creep characteristics of Cu-2wt%Sn alloy in the solid solution region[J]. Physics B, 2004, 344(1—4): 443—450.

[7] Casalino G, Ludovico A D, Dattoma V, *et al*. The use of discharge energy for rapid welding[M]. B Katalinic (Ed), DAAAM Int Scientific Book, 2003.

[8] Xu J F, Zhai Q Y, Jiang Y. Energy-storage welding connection characteristics of y rapidly solidified Cu-Co alloy foils[J]. Transactions Nonferrous Mettals Society of China, 2004, 4(14): 785—789.

[9] 翟秋亚, 徐锦锋. Cu-Sn 合金急冷箔储能焊接头的形貌特征与形成机制[J]. 金属学报, 2005, 41(7): 755—758.
Zhai Qiuya, Xu Jinfeng. Morphological characteristic and formation mechanism of joint of melt-spun Cu-Sn alloy foils by capacitor discharge welding[J]. Acta Metallrugica Sinica, 2005, 41(7): 755—758.

[10] 翟秋亚, 杨金山, 徐锦锋, 等. 急冷 Cu-Sn 快速凝固焊接接头组织特征[J]. 焊接学报, 2009, 30(4): 49—52.
Zhai Qiuya, Yang Jinshan, Xu Jinfeng, *et al*. Microstructal characteristic of joint of quenched Cu-Sn alloy foils by rapid solidification welding[J]. Transactions of the China Welding Institution, 2009, 30(4): 49—52.

作者简介: 翟秋亚, 女, 1963 年出生, 工学博士, 副教授. 主要从事先进材料焊接方面的研究. 发表论文 50 余篇.

Email: qiuyazhai@xaut.edu.cn

[上接第 52 页]

[6] 李福义. 液压技术与液压伺服系统[M]. 哈尔滨: 哈尔滨工程大学出版社, 1995.

[7] Khan H, Seraphin C Abou, Sepehri N. Nonlinear observer-based fault detection technique for electro-hydraulic servo-positioning systems[J]. Mechatronics, 2005, 15: 1037—1059.

作者简介: 银东东, 男, 1983 年出生, 硕士研究生. 主要从事线性摩擦焊接设备的控制研究. 发表论文 1 篇.

Email: ydd02142@163.com

(FZ) and the average micro-hardness value is 447HV when heat input E= 135 kJ/m is utilized. With heat input increasing to 150 kJ/m, the number of α' phase decreases in FZ, short acicular $\alpha+\beta$ phase become coarser in heat-affected zone(HAZ) of TC11, coarse β grains become larger in HAZ of Ti-24Al-15Nb-1.5Mo and the average micro-hardness value drops to 402HV. The result is attributed to the changed content of alloy elements and lower cooling velocity caused by increasing heat input. The content of element Ti, Al and Nb is changed abruptly in the boundary of the joint, but these elements evenly distribute in each zone and hardly diffuse.

Key words: electron beam welding; dual alloy; heat input; fine texture; microstructure

Microstructural characterization of TC4/Cu/ZQSn10-2-3 diffusion bonded joints ZHAO He, CAO Jian, FENG Jicai (State Key Laboratory of Advanced Welding Production Technology, Harbin Institute of Technology, Harbin 150001, China). p 37—40

Abstract: The experimental investigation on the diffusion bonding of TC4 to ZQSn10-2-3 was carried out in vacuum. $CuSn_3Ti_5$, Cu_3Ti and rich-Pb layer were formed at the interface zone. The maximum joint strength was 102 MPa. Brittle fracture was explored after shear test, and occurred proximity to ZQSn10-2-3 side. Using copper as the interlayer, element Sn and Pb can be avoid diffusing from ZQSn10-2-3 to TC4. Then there were little $CuSn_3Ti_5$ in the interface. Fracture had certain plasticity, and the maximum strength of joint was 196 MPa. The optimum bonding parameters were: bonding temperature T= 830 ℃, bonding pressure p= 10 MPa and bonding time t= 30 min.

Key words: titanium alloy; tin-bronze; diffusion bonding; copper interlayer

Intelligent process modeling of robotic plasma spraying based on multi-layer artificial neural network XIA Weisheng[1,2], ZHANG Haiou[2], WANG Guilan[1], YANG Yunzhen[1] (1. State Key Laboratory of Material Processing and Die & Mould Technology, Huazhong Universiry of Technology, Wuhan 430074, China; 2. State Key Laboratory of Digital Manufacturing Equipment and Technology, Huazhong University of Science & Technology, Wuhan 430074, China). p 41—44

Abstract: The implementation of multi-layer artificial neural networks (ANNs) in robotic plasma spraying was discussed and an intelligent process model was constructed to fully describe the relationships between process parameters and coating properties. Influences of plasma arc current, spray distance, robot scanning space and scanning velocity on coating properties, i. e. residual stress and porosity, were systematically studied based on the present model. Prediction can be effectively carried out after the learning of the experimental database. Theoretical analysis shows the prediction results agree well with the experiments. It is favorable to fully investigate the complex and nonlinear relationships between processing parameters and coating properties as well as to overcome the limited information indicated by the discrete variable in the processing results.

Key words: robotic plasma spraying; artificial neural network; intelligent model; residual stress; porosity

Kinematics and track amendments of intersecting pipe welding robot DU Hongwang[1,2], WANG Zongyi[2], LIU Shaogang[1], ZHAO Yanan[1] (1. College of Mechanical & Electrical Engineering, Harbin Engineering University, Harbin 150001, China; 2. College of Automation, Harbin Engineering University, Harbin 150001, China). p 45—48

Abstract: According to the welding particularity on the junctions of intersecting pipe, the 4 degrees of freedom suspended welding robot was developed and mechanical structure of the body was introduced. Based on the relation of the joints, the kinematics modeling was established with the method of D-H (Denavit-Hartenberg). To overcome the size error and processing error and welding distortion, the welding track was taught in order to ensure welding quality, and then theory track was amended by the linear interpolation. According to the kinematics modeling, the simulation was carried out with SemMechanic. The results of experiments show that the welding quality meet the requirements actually.

Key words: welding robot; kinematics; teaching; linear interpolation

Dynamical simulation on the pressure response of load system of linear friction welding machine YIN Dongdong, DU Suigeng, YU Longqi, MA Yunfeng (Key Laboratory of Ministry of Education for Contemporary Design and Integrated Manufacturing Technology, Northwestern Polytechnical University, Xi'an 710072, China). p 49—52, 56

Abstract: In order to study the closed-loop control qualities of the electro-hydraulic servo load system of the linear friction welding machine on the slipway pressure, closed-loop transfer function of the pressure for the electro-hydraulic servo load system was established according to the relationship between input and output variables, a simulation model was established according to the transfer function and the simulation was carried out. In order to validate reliability of the simulation result, a frequency characteristics experiment of pressure was implemented under closed-loop control, and the system pressure's affect on the pressure's closed-loop response characteristics was specially analyzed. The results show as follows: the emulational and experimental results are anastomosing; the electro-hydraulic servo load system is a second-order inertial & first-order differential link for closed-loop pressure control, the system frequency width is large, and the system stability is high; pressure's closed-loop dynamic response characteristics can be improved by promoting the system pressure.

Key words: linear friction welding machine; electro-hydraulic servo system; dynamic quality; simulation

Study on rapid solidification welding techniques of quenched Cu-Sn alloy foils ZHAI Qiuya, YANG Jinshan, XU Jinfeng, GUO

Xuefeng (School of Materials Science and Engineering, Xi' an University of Technology, Xi' an 710048, China). p 53—56

Abstract: The rapid solidification welding of quenched Cu-Sn alloy foils with the thickness of 40—60μm was conducted by a micro-type capacitor discharge welding machine, and the effects of welding parameters on microstructural morphology and mechanical properties of joint were researched. The results indicate that welding voltage and electrode pressure have obvious influence on the shear strength of joint under fixed capacitance. With the increase of Sn content, the welding voltage needed decreases and electrode pressure rises accordingly. The favorable welding parameters are U= 90 V, F= 11 N for Cu-7%Sn alloy and U= 85 V, F= 11.5 N for Cu-13.5% Sn alloy. The main welding defect is porosity. With decreasing of welding voltage and increasing of electrode pressure, the joint cooling rate increases and the pore nucleation rate decreases. Meanwhile, the growth, mergence and migration of porosities are suppressed, resulting in the decrease of porosity forming tendency.

Key words: quenched Cu-Sn alloy; alloy foil; rapid solidification weld; shear strength

Fast transform ultra-sonic pulse TIG welding QI Bojin, XU Haiying, ZHOU Xingguo, HUANG Songtao (School of Mechanical Engineering and Automation, Beijing University of Aeronautics Astronautics, Beijing 100191, China). p 57—60

Abstract: A current fast transform ultra-sonic pulse TIG power source based on new type IGBT topology was developed. The supremest output pulse current frequency is 30 kHz. The pulse current change rate is up to 50 A per microsecond. 0Cr18Ni9Ti austenitic stainless steel was welded by this fast transform ultra-sonic pulse TIG welding and conventional DC TIG welding respectively. These joints were analyzed by X-radial check-up, tensile strength and specific elongation detection, optical-microscope and scanning electron microscope to study the difference between joints welded by different welding technologies. The result shows that fast transform ultra-sonic pulse TIG welding can refine grain and narrow the width of the coarse grain zone. These indicate that welding quality is improved by introducing fast transform ultra-sonic pulse TIG welding technology.

Key words: ultra-sonic pulse; grain refinement; welding joint

Microstructure and mechanical property of 93W/Ni/QSn4-3 joint welded by diffusion bonding SU Xiaopeng[1], LUO Guoqiang[1,2], SHEN Qiang[1], WANG Chuanbin[1], ZHANG Lianmeng[1] (1. State Key Laboratory of Advanced Technology for Materials Synthesis and Processing, Wuhan University of Technology, Wuhan 430070, China; 2. Laboratory for Shock Wave and Detonation Physics Research, Southwest Institute of Fluid Physics, CAEP, Mianyang 621900, Sichuan, China). p 61—64

Abstract: The 93W/Ni/QSn4-3 joint was prepared by diffusion bonding at vacuum using pure nickel foil as interface layer. The microstructure and composition were characterized by SEM and EPMA. The tensile strength of joint was also measured. The test results show that Ni foil improves the tensile strength of 93W/Ni/QSn4-3 joint. The thickness of Ni interlayer becomes thiner obviously because of the diffusion layer between Ni element of Ni foil and W and additional elements of 93W alloy, as well as the gradient layer of Ni and Cu elements. Solution reactions between Ni element of Ni foil and Cu element of QSn4-3 alloy, W and additional elements of 93W alloy achieve the joint of 93W/Ni/QSn4-3, that is why tensile strength of 93W/Ni/QSn4-3 joint welded is improved.

Key words: diffusion bonding; tungsten alloy; tin-bronze (QSn4-3); nickel foil

Properties and microstructures of Fe-Cr coating with high boron by plasma cladding process MA Hu, WU Yuping, WANG Guotong (School of Materials Science and Engineering, Hehai University, Nanjing 210098, China). p 65—68

Abstract: A harden coating of Fe-Cr based alloy, containing high boron, was produced on midium carbon steel plate by plasma cladding process. The phases, microstructures and microhardness of the cladding coating were investigated by Scanning Electron Microscopy (SEM), X-ray Diffractometer (XRD), Energy-dispersive Spectroscopy (EDS) and microhardness tester. The chief phases of the cladding coating are γ-Fe(Ni) and Fe_2B. The microstructures of cladding coating were consisted of Fe_2B with shapes of equilateral L or lath and eutectic of γ-Fe(Ni) and borides, and the eutectic presented itself with lamella or rosette shape. An excellent metallurgical interface between the coating and the substrate appeared. The microstructures of the layer near the interface exhibit fan-shaped or dendritic structure. The microhardness value of the cladding coating was 1 100—1 400$HV_{0.2}$ and was about 4 times of the substrate (290$HV_{0.2}$). The microhardness of the substrate near the interface increased to 600$HV_{0.2}$ because of quenching.

Key words: plasma cladding coating; microstructure; microhardness; 45 steel; heat-affected zone

Effect of restraint condition on hot cracking during welding of 2A12T4 aluminum alloy LI Jun[1,2], YANG Jianguo[1], YAN Dejun[1], FANG Hongyuan[1] (1. State Key Laboratory of Advanced Welding Production Technology, Harbin Institute of Technology, Harbin 150001, China; 2. Guangzhou Research Institute of Non-ferrous Metals, Guangzhou 510651, China). p 69—72

Abstract: A simple and effective experimental method was adopted to investigate the effects of restraint force and restraint distance on hot cracking tendency during welding of 2A12T4 aluminum alloy on the common rigid welding fixture. Experimental results show that, under the condition of keeping restraint distance unchanged, the rate of hot cracks decreases gradually with increase of restraint force and finally well reaches a stable value when the reatraint force is great enough. Keeping the restraint force unchanged, the rate of hot cracks increases with increase of restraint distance. The influence of restraint condition on tendency of hot cracking through effect-